ANL-7926
Reactor Technology

ARGONNE NATIONAL LABORATORY
9700 South Cass Avenue
Argonne, Illinois 60439

ACTIVATION-RATE MEASUREMENTS IN THE ZPR-3 MOCKUP CRITICAL EXPERIMENTS

Part II. Measurements of Foil-activation Rates in Assembly 61 of ZPR-3 Mockup of EBR-II with a Nickel Reflector

by

R. R. Heinrich, N. D. Dudey, R. J. Popek,
R. P. Larsen, and R. D. Oldham

Chemical Engineering Division

March 1972

Part I was ANL-7781

DISCLAIMER

TABLE OF CONTENTS

LIST OF FIGURES

LIST OF TABLES

LIST OF TABLES (Continued)

ACTIVATION-RATE MEASUREMENTS IN THE ZPR-3 MOCKUP CRITICAL EXPERIMENTS

Part II. Measurements of Foil-activation Rates and Fission Yields in Assembly 61 of ZPR-3 Mockup of EBR-II with a Nickel Reflector

by

R. R. Heinrich, N. D. Dudey, R. J. Popek,
R. P. Larsen, and R. D. Oldham

ABSTRACT

This report is the second in a series that will discuss activation-rate measurements conducted in the ZPR-3 critical facility in mockup experiments designed to simulate various configurations of EBR-II. The primary objective of the reports is to describe these measurements and to present the data in a useful form. This report describes the activation-rate measurements conducted in Assembly 61 of ZPR-3. The study consisted of two experiments. The first experiment was designed to provide activation-rate data for dosimetry purposes, i.e., data for characterizing the irradiation environment in terms of reaction rates, neutron flux and neutron spectrum, and for defining the effects of heterogeneity within the assembly. The second experiment was designed to provide data from which fast-neutron fission yields of several short- to intermediate-lived fission products could be established. The measurements were made using a Ge(Li) detector and solid-state fission-track recorder. Both experiments involved irradiations of foils near the center of the reactor core, near the core-reflector interface, and within the nickel radial reflector, which in Assembly 61 replaced the uranium blanket of Assembly 60. The data on fission yields and reaction rates are presented, intercompared, and also compared with the results from another activation-rate experiment conducted by an independent group.

I. INTRODUCTION

This is the second report in a series describing the results of foil-activation-rate measurements conducted in the ZPR-3 critical facility mocked up to simulate various possible EBR-II configurations. The first report[1] described work in Assembly 60 of ZPR-3. The present report describes measurements conducted in Assembly 61 of ZPR-3. The two assemblies differed in the following ways. In Assembly 61, a nickel reflector was substituted for a portion of the depleted uranium blanket in Assembly 60, and the ^{235}U content of the core was slightly decreased.

Only those aspects of the Assembly 61 experiments which differed from Assembly 60 will be presented, since the objectives, irradiation conditions, activation-rate measurements, and data processing are all similar to those described in the preceding report[1] of this series. The specific objectives of the Assembly 61 experiment were to provide both reaction-rate results and fission-yield data for a nickel-reflected configuration that could be compared with those obtained with a configuration in which a radial blanket of depleted uranium was used (Assembly 60) and those obtained with a configuration in which a stainless steel reflector was used (Assembly 62). Measurements made in Assembly 62 and 63 will be described in a subsequent report in this series.

II. DESCRIPTION OF IRRADIATIONS IN ASSEMBLY 61

Assembly 61, Final Transition Step, was identical to Assembly 60 with two exceptions. Firstly, a four-drawer-thick region of the uranium blanket immediately adjacent to the core was replaced by a four-drawer-thick region of nickel. The final reference loading of Assembly 61 is shown in Fig. 1. The first four rows surrounding the core were designated as the nickel-rich reflector region, R5. This region was reflected, top and bottom, by a stainless steel-rich reflector region, R6, which extended the height of the top and bottom axial reflectors. The radial blanket region, R7, was identical to Assembly 60. Secondly, the ^{235}U content in the core was reduced to maintain a critical volume which more closely represented EBR-II. This was accomplished by replacing a 1/32-in.-thick column of 93% enriched uranium in Assembly 60 with a 1/32-in.-thick column of natural uranium in Assembly 61. The reference critical loading was 208.58 kg of ^{235}U. The composition of the modified core is listed in Table I. A more detailed description of Assembly 61 appears in Ref. 2 and 3. Figure 1 illustrates the front view of the Half No. 1 matrix in which the irradiations took place. Figure 2 illustrates a front view of the plate configuration within both the core and the reflector zone, R5.

The foil packets in Assembly 61 were similar to those used in Assembly 60 with only minor variations. Five types of foil sets were prepared; these are designated D, Y, A, NS, and F in Fig. 1. The D and Y foil sets were analyzed by this laboratory while the A, NS, and F foil sets were analyzed by the Applied Physics Division of ANL-West. Each foil type was irradiated in the same matrix position as its counterpart in Assembly 60. The dosimetry (D) foil packets were located near the core center (0-15),

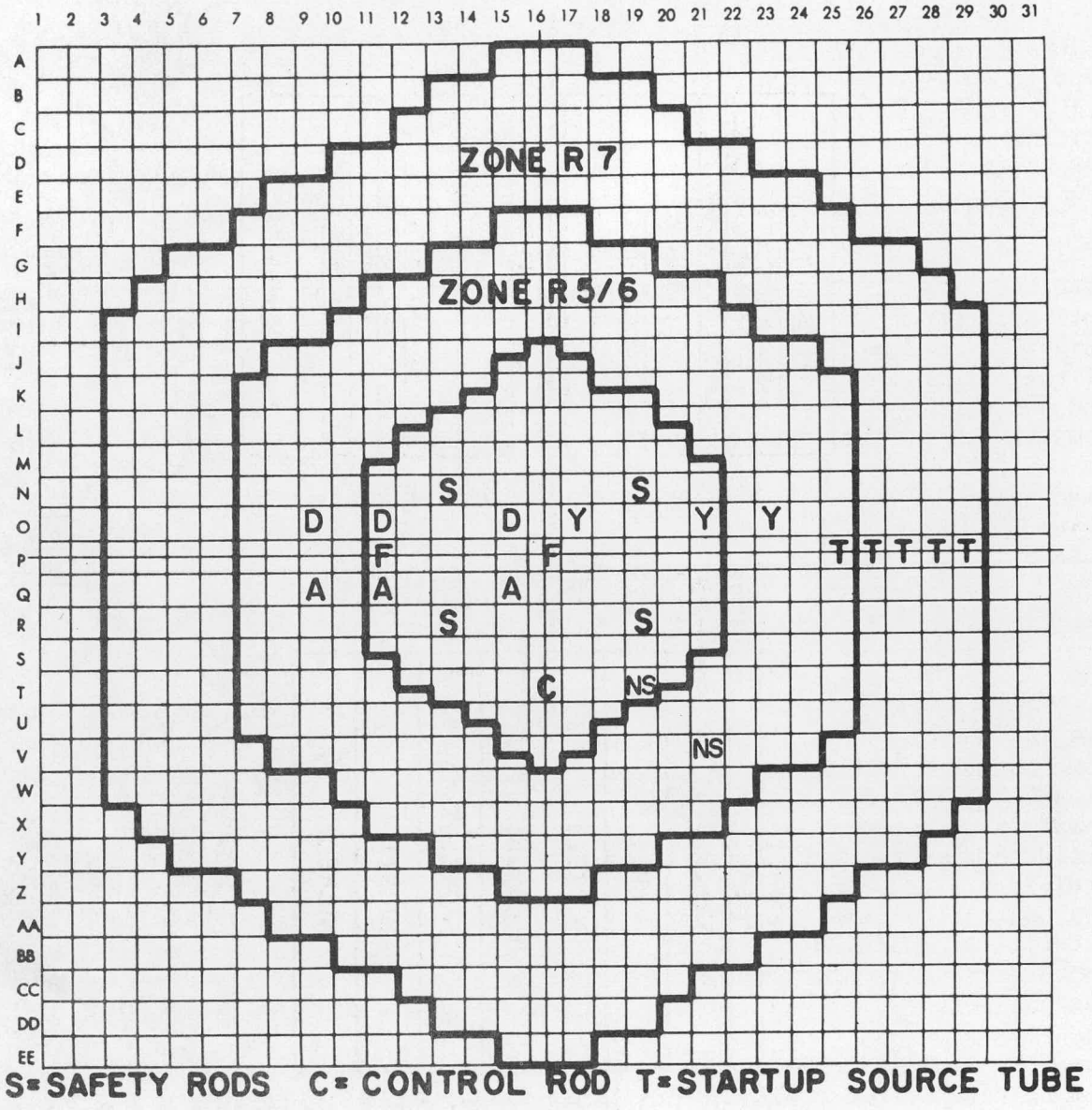

Fig. 1. Matrix Pattern and Foil-packet Locations in Assembly 61 (Vertical Cross Section of Half No. 1)

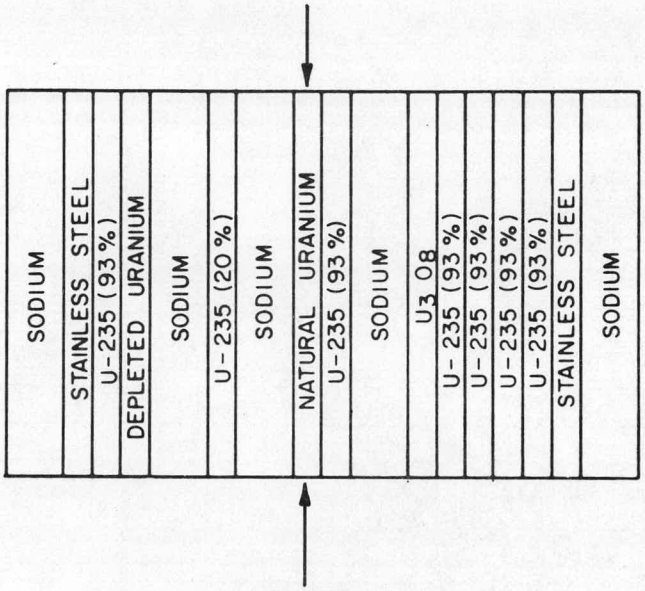

Fig. 2. Plate Configurations and Composition of the Core and Nickel-rich Reflector of Assembly 61

TABLE I. ZPR-3 Assembly 61, Modified Core Compositions
(Units: 10^{24} atoms/cc)

Element	Core; Half 1	Core; Half 2	Core; Average[a]
^{235}U	0.005064	0.005098	0.005080
^{238}U	0.005055	0.005051	0.005053
Na	0.01017	0.01052	0.01033
Fe	0.01323	0.01353	0.01337
Cr	0.00340	0.00347	0.00343
Ni	0.00148	0.00151	0.00149
Mn	0.000171	0.000174	0.000172
Si	0.00013	0.00013	0.00013
O	0.002137	0.002132	0.002135

[a]This represents weighted core average; i.e., 7.03 in./13.06 in. = 0.5383 Half 1, and 6.03 in./13.06 in. = 0.4617 Half 2.

on the core side of the core-reflector interface (0-11), and in the radial reflector (0-9). The core packet contained 1.97-in. square metal foils of uranium-235, uranium-238, gold, nickel, and aluminum. The core-reflector interface packet and the radial reflector packet contained all of the above materials except aluminum. Aluminum was added to the core packet of Assembly 61 to evaluate the usefulness of the $^{27}Al(n,\alpha)$ reaction as a dosimetry monitor for critical assembly. The weights and thicknesses of each of the foils are listed in Table II. The isotopic compositions of the ^{235}U and ^{238}U foils are given in Table III.

TABLE II. Weights and Thicknesses of Foils in Dosimetry Packets

Monitor	Core		Core-reflector Interface		Radial Reflector	
	Thickness (in.)	Wt. (g)	Thickness (in.)	Wt. (g)	Thickness (in.)	Wt. (g)
Nickel	0.010	5.6	0.010	5.6	0.010	5.6
Uranium-235	0.006	6.6	0.006	6.7	0.006	6.7
Gold	0.0002	0.24	0.0006	0.70	0.0006	0.70
Uranium-238	0.010	11.7	0.010	11.7	0.010	11.2
Aluminum	0.010	1.7	-	-	-	-

TABLE III. Isotopic Compositions of ^{238}U, ^{235}U, ^{239}Pu, ^{242}Pu, and ^{237}Np Foils in Dosimetry and Fission-yield Packets

Material	Dosimetry Foils		Fission-yield Foils	
^{238}U	99.78%	^{238}U	99.78%	^{238}U
	0.22%	^{235}U	0.22%	^{235}U
^{235}U	93.10%	^{235}U	93.12%	^{235}U
	6.90%	^{238}U	0.96%	^{234}U
			0.32%	^{236}U
			5.59%	^{238}U
^{239}Pu			94.61%	^{239}Pu
			5.06%	^{240}Pu
			0.31%	^{241}Pu
			0.02%	^{242}Pu
^{242}Pu			99.74%	^{242}Pu
			0.14%	^{241}Pu
			0.11%	^{240}Pu
			0.01%	^{239}Pu
			0.01%	^{238}Pu
^{237}Np			100%	^{237}Np

A modification was also made to the interface and reflector packets of Assembly 61. Since the nickel-rich reflector results in considerable spectral softening and the $^{197}Au(n,\gamma)$ reaction has a large resonance at ~5 eV, the magnitude of resonance self-shielding in the gold monitor foils could be significant. To examine this effect, we added three 0.2-mil-thick gold foils to the interface and relfector packets, whereas only one gold foil was irradiated in the core packet.

Each uranium foil was individually wrapped in commercial-grade aluminum foil (0.0008 in. thick) to contain any recoil fission fragments and to prevent cross contamination between the uranium foils. The individual foils were stacked in the order given in Table II and then wrapped together in the same type of aluminum foil to constitute an individual packet. The total weight of aluminum per packet was about 1 g. An assembled packet showing its front-view identification and side-view foil orientation within the drawer is illustrated in Fig. 3. The packets were inserted into their respective drawers perpendicular to the plates and about 1-in. from the physical mid-plane of the split-table assembly.

The objective of the Y-foil experiments, as in the case of Assembly 60 experiments, was to determine fission-product yields from several fissioning species. The yield data from the softer neutron spectra of Assembly 61,

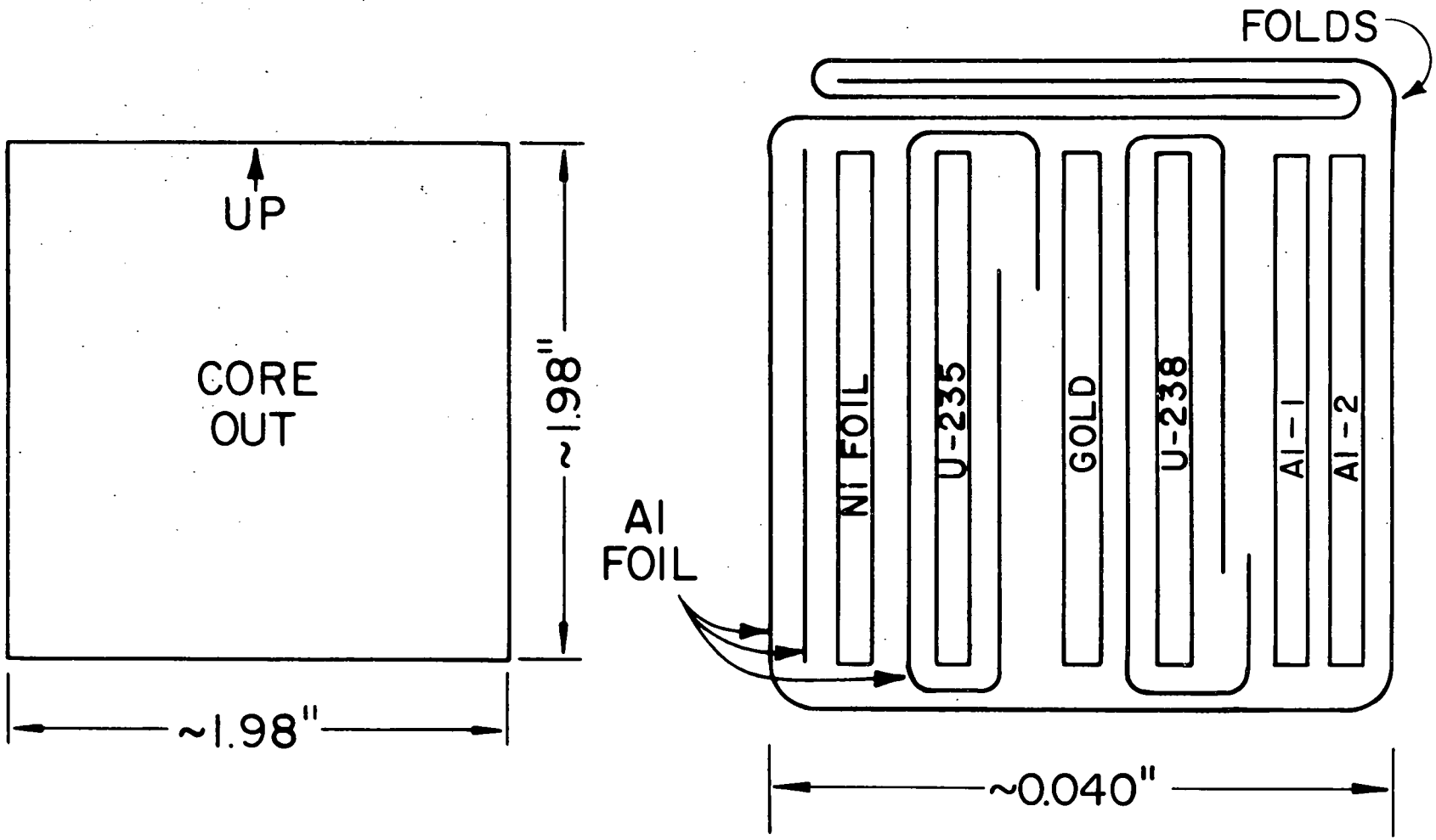

Fig. 3. Cutaway Front and Side View of Dosimetry Foil Packet

together with the yield data from the Assembly 60 experiments, provide a systematic means for determining the energy (spectral) dependence of several fission-product yields over the range of neutron energies expected to be present in fast breeder reactors. These data can also be applied to defining the energy spectra found in EBR-II between the core and the extreme outer portions of the axial and radial blankets. The technique used to determine fission yields involves exposing nanogram amounts of fissile material in contact with mica fission-track recorders to determine the absolute number of fissions per nanogram of fissile material and simultaneously irradiating massive amounts ($\sim$1 g) of the fissile material from which the gamma-active fission products are measured. This solid-state track-recorder (SSTR) technique is described more fully in Ref. 1.

The Assembly 61 fission-yield measurements differed slightly from those in Assembly 60 in that foils of ^{242}Pu and ^{237}Np were added to the ^{235}U, ^{238}U, and ^{239}Pu foils in the Y packets in Assembly 61. In addition, the orientation of the packets relative to the drawer plates was altered. Figure 4 illustrates the physical orientation of the massive foils and the SSTRs in the holder. In Assembly 61, the long strips were aligned parallel to the fuel plates as opposed to the perpendicular alignment in Assembly 60. The change in orientation was made to minimize the heterogeneity effects on the strips due to the drawer-plate structure in the assembly by providing a more uniform fluence and spectral distribution along each strip of material. The Y packets were irradiated on the right side of Half 1 in positions symmetric with the D packets (see Fig. 1). The sample identification schemes of both the mica fission-track recorders and the massive foil samples are shown in Figs. 5, 6, and 7 for the core, interface, and reflector packets, respectively. The isotopic compositions of the Y-foil samples is given in Table III.

The foil-activation experiments designated A, F, and NS in Fig. 1, which were conducted by the Applied Physics Division of ANL-West, have been reported elsewhere.[4-5] The A and F foil sets consisted of 0.5-in.-dia by 0.005-in.-thick foils of ^{235}U, ^{238}U, aluminum, tungsten, gold, indium, and nickel. The A foils were positioned between selected plates, i.e., parallel to the plates, within a drawer in an assembly position symmetric with the D and Y foils (see Fig. 1). The F experiments were designed to examine spectral effects due to the structural boundaries. The NS experiments were planned to provide activation-rate data from which neutron spectral information might be deduced. Additional information on the A, F, and NS experiments is given in references 4 and 5.

All foil-activation samples were irradiated simultaneously in ZPR-3 for 60 min at a nominal power level of 600 W. The irradiation terminated at 1111 MDT on June 4, 1970. The D and Y packets were shipped to Argonne-Illinois for analysis immediately after the irradiation.

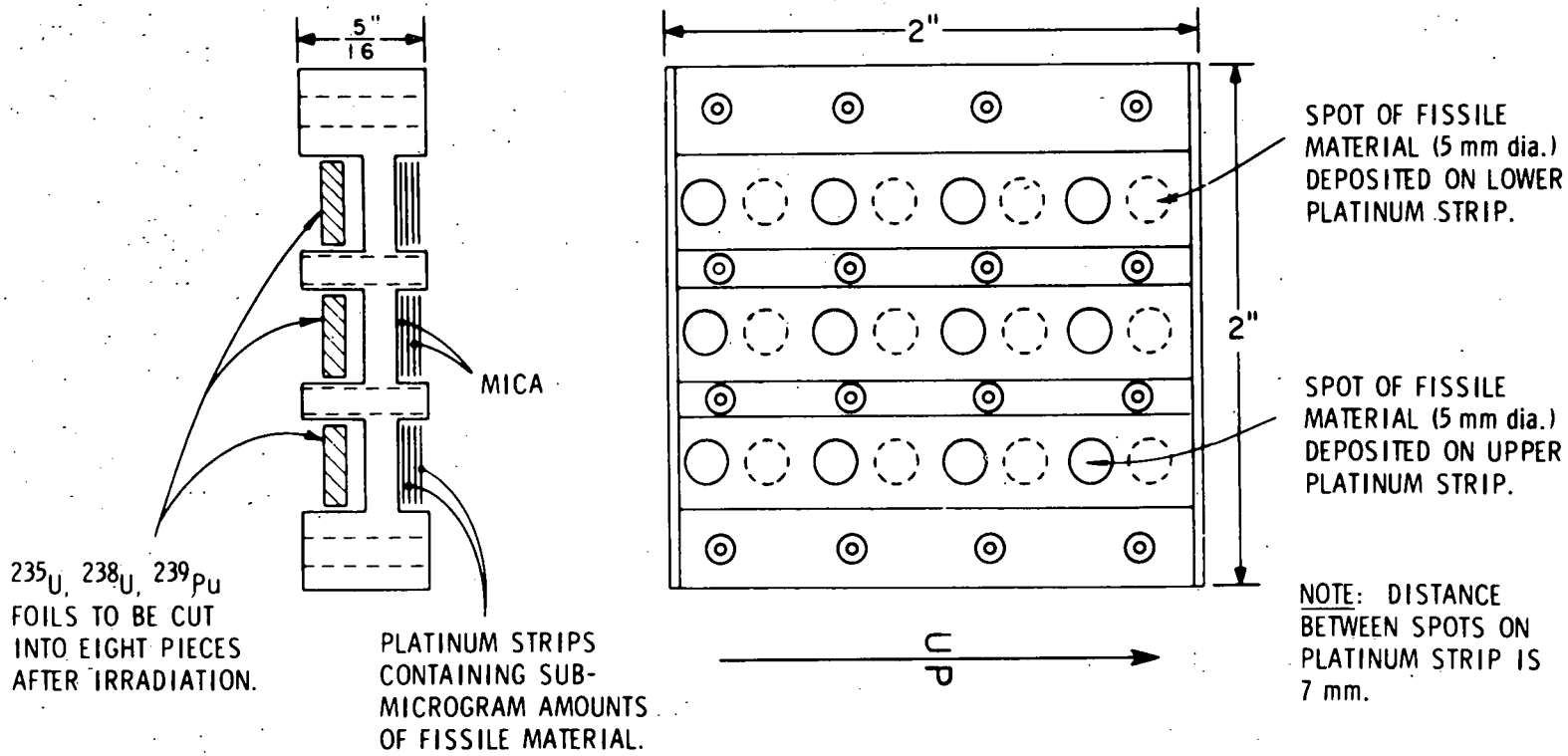

Fig. 4. Cutaway End and Front View of Fission-yield Packets

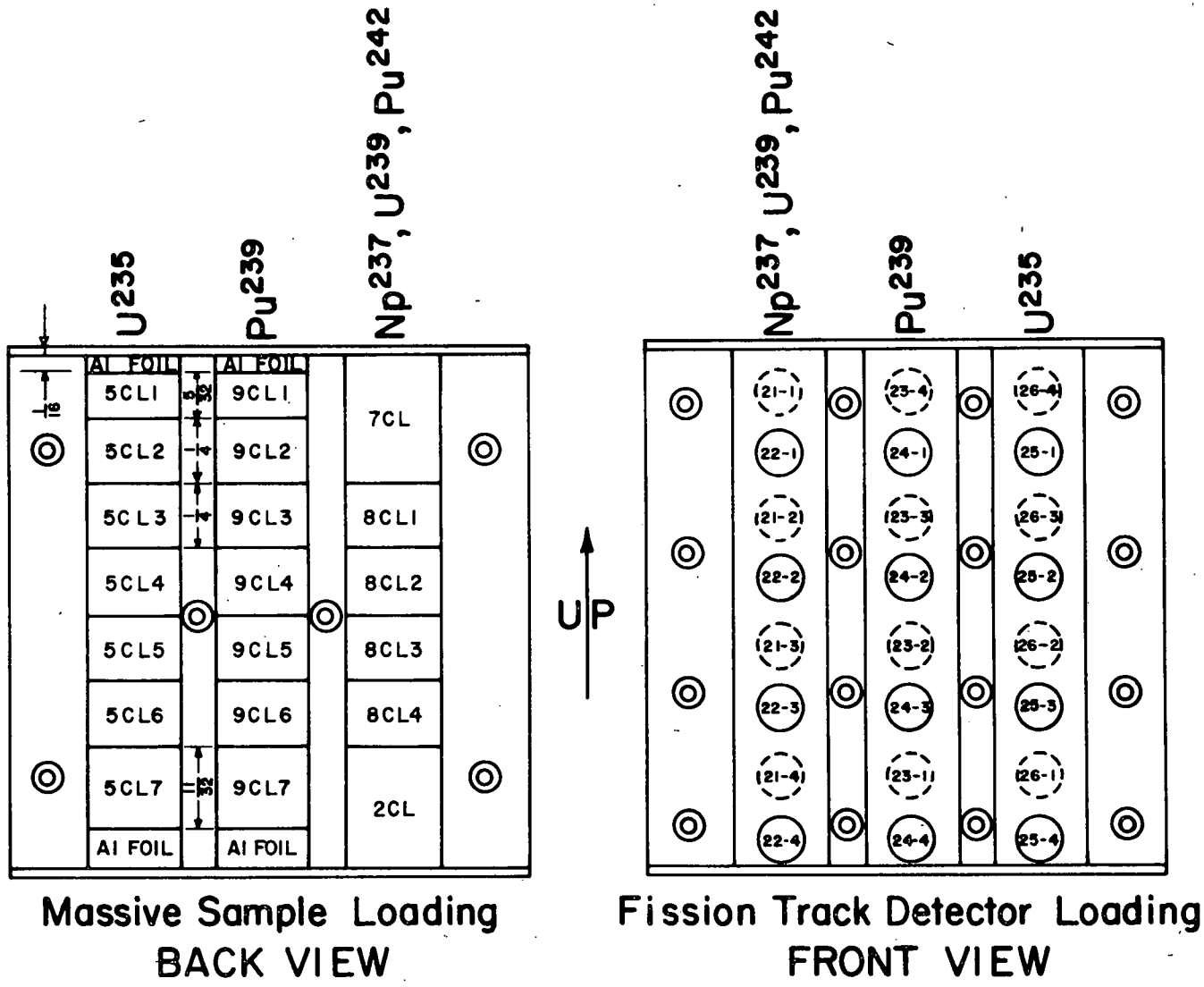

Fig. 5. Sample Identification Scheme for Fission-yield Core Packet

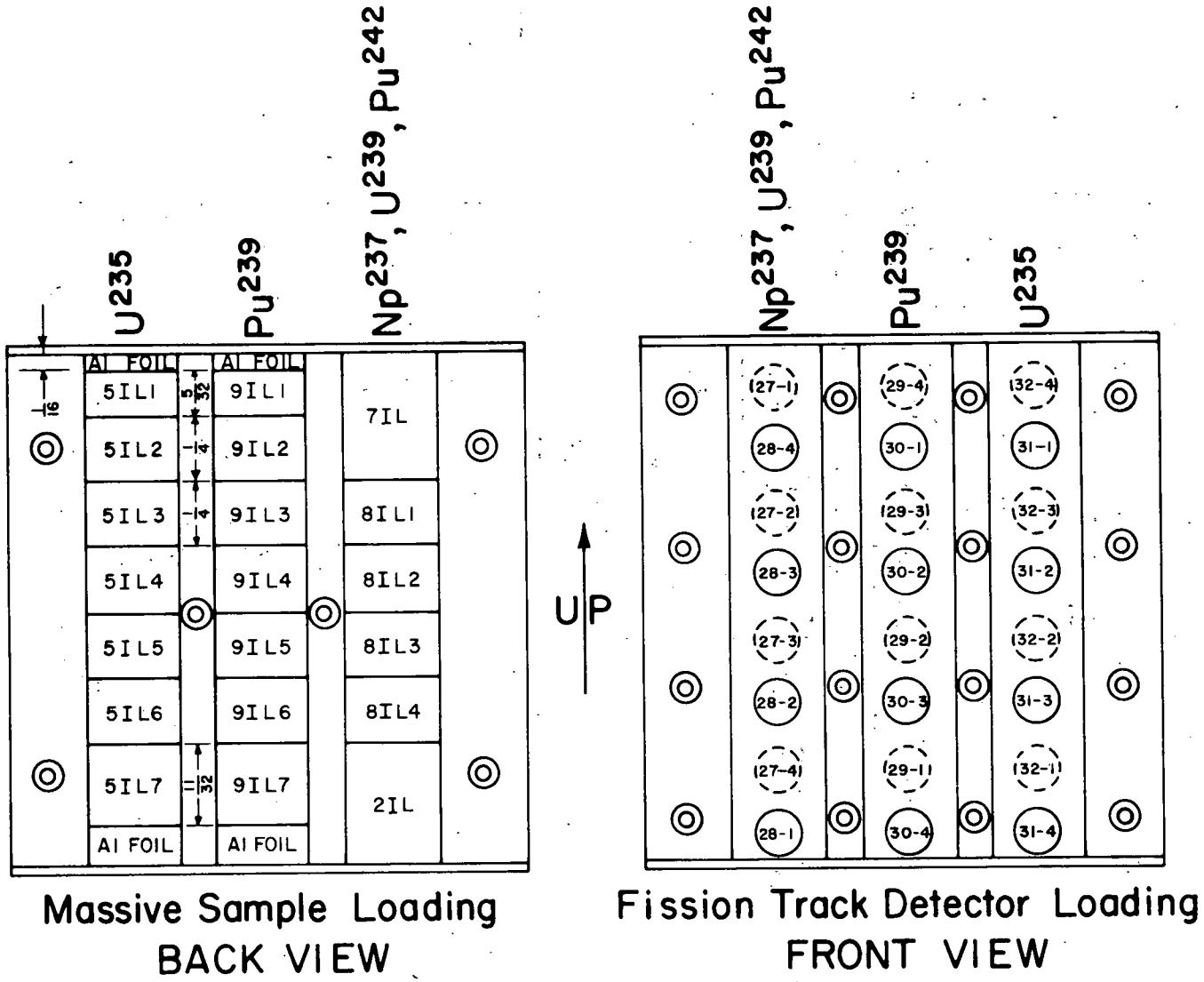

Fig. 6. Sample Identification Scheme for Fission-yield Core-interface Packet

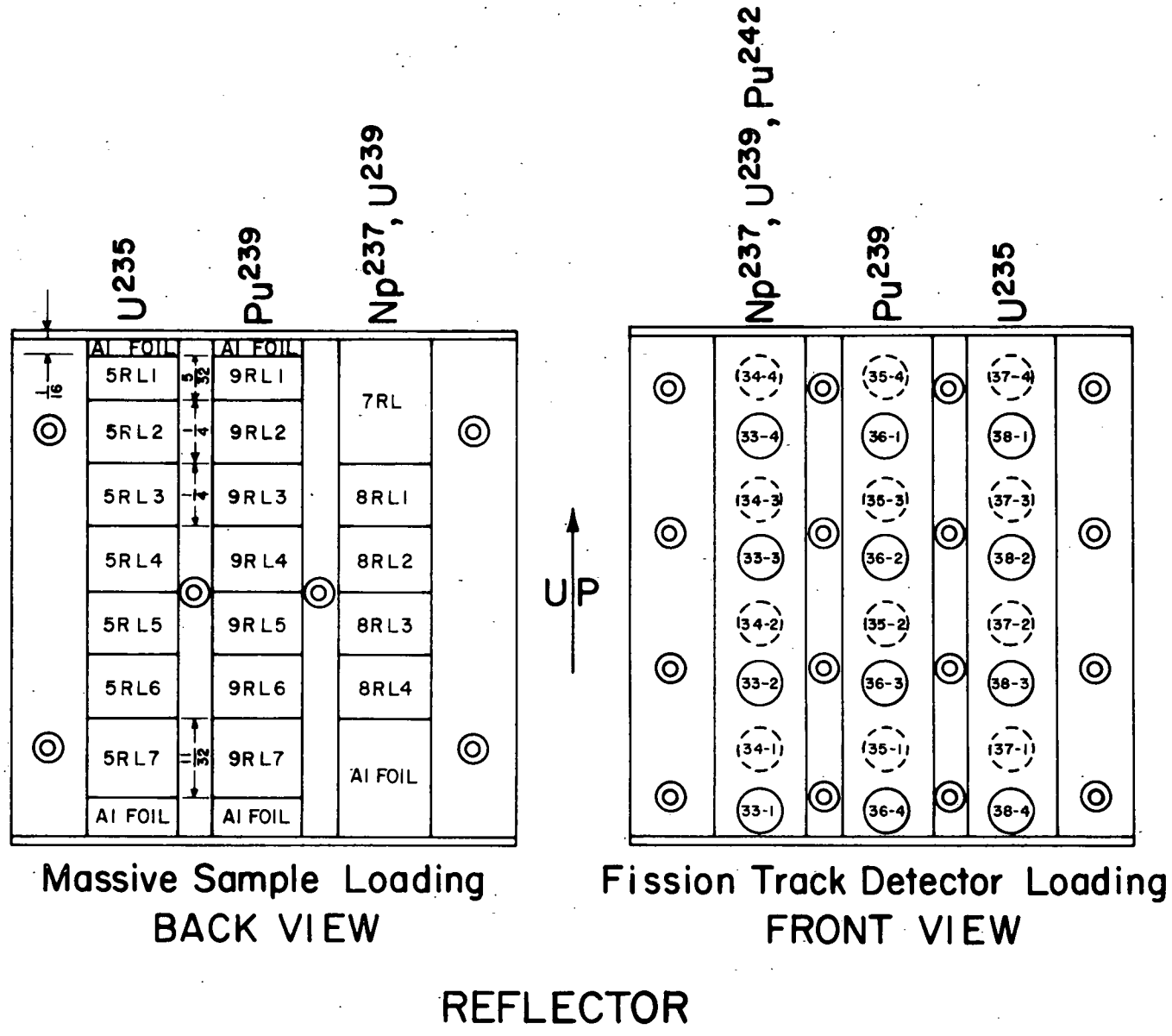

Fig. 7. Sample Identification Scheme for Fission-yield Reflector Packet

III. EXPERIMENTAL ANALYSIS OF THE IRRADIATED SAMPLES

A. Preparation of the Samples for Counting

Upon receipt of the samples, the aluminum wrapping was removed from the D packets and the 2-in. by 2-in. foils were cut into smaller pieces for counting. The dimensions of the cut pieces and their identification are shown in Fig. 8. The cutting pattern was designed to maximize the heterogeneity effects upon the foils which resulted from the plate composition of the assembly drawers and to correlate these effects with similar measurements in Assemblies 60 and 62 as well as with the results obtained with the A-foils measured by the Applied Physics group. In the case of the gold samples, the number preceding the symbol Au differentiates the foils in each packet; thus, number 1 designates the foil in the packet closest to the core midplane, 2 designates the middle foil, and 3, the gold foil farthest from the reactor midplane.

The fission-yield, Y samples were handled similarly. The platinum plates and mica fission-track recorders were first removed and stored for later analysis. Reference 1 describes the analytical procedures used. The fissile foil strips were cut into 1/4-in. sections according to the patterns presented in Figs. 5-7. Of these sections, those numbered 5CL-7, 5IL-7, 5RL-7, 8CL-1, 8IL-1, 8RL-1, 9CL-7, 9IL-7, and 9RL-7 were reserved for radiochemical determinations of the ^{99}Mo and ^{140}Ba contents. The remaining sections were mounted for gamma-counting.

The cut pieces, both D and Y, were individually weighed and those that were to be gamma-counted were mounted on 1/16-in.-thick aluminum plates. Several of the 2-in.-long D pieces were cut into smaller pieces and mounted side by side on the aluminum mounting plate. This resulted in a more acceptable counting geometry than would have been obtained with long thin strips. The aluminum wrapping foils that had been wrapped around the D samples were mounted adjacent to the fissile piece(s) for counting. The weights of the Y-samples, both those adjacent to the mica and the massive samples, and their identification numbers are presented in Tables IV, V, and VI for ^{235}U, ^{238}U, ^{239}Pu, ^{242}Pu, and ^{237}Np. The weights and sample numbers for the D samples are given in Tables VII, VIII, and IX.

B. Gamma-counting of the Irradiated Samples and Data Analysis

Gamma-counting of the samples was begun about 28 hr after the end of the irradiation. The Ge(Li) and NaI(Tl) detector systems, counting philosophy, and data reduction codes were identical to those used in the Assembly 60 measurements. Also, all considerations related to corrections of the data and analysis of errors are fully discussed in Ref. 1. The aluminum samples, which were not included in the Assembly 60 experiments, were counted on the NaI(Tl) detector system.

The experience gained from the Assembly 60 measurements enabled us to improve the Assembly 61 measurements by incorporating several minor changes. The most significant change was to spread out the pieces of a given sample over a larger area instead of stacking the pieces as had been done previously. This required a somewhat larger correction for counting geometry, but

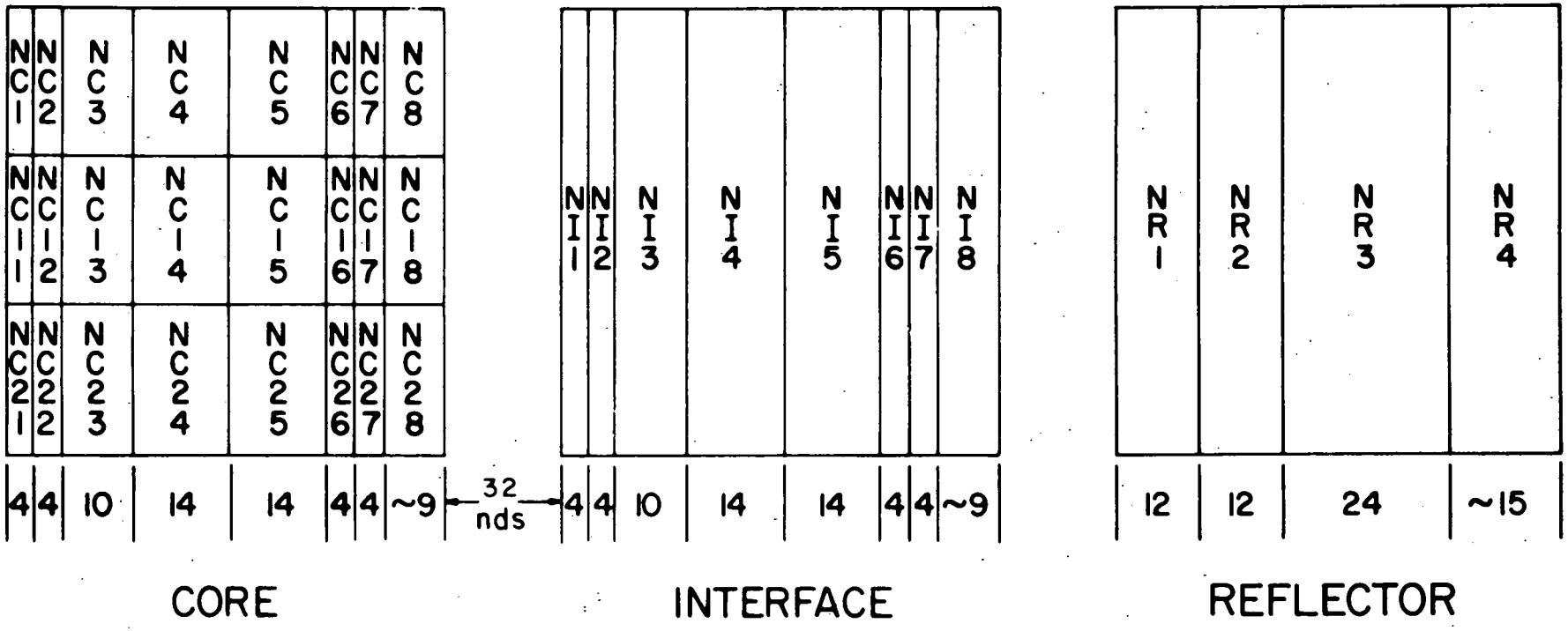

Fig. 8. Cutting Diagram and Sample Identification Scheme for Dosimetry Packets

TABLE IV. Weights of Uranium Samples in the Fission-yield Packets

^{235}U Foil Samples		^{235}U Track Recorder Samples	
Sample No.	Weight, mg	Sample No.	Weight, ng
5RL1	-	37-4	14.96
5RL2	507.5	38-1	4.19
5RL3	559.4	37-3	18.42
5RL4	549.1	38-2	4.59
5RL5	482.1	37-2	19.25
5RL6	495.2	38-3	4.63
5RL7 }	-	37-1	7.73
5RL7 }		38-4	4.70
5IL1	-	32-4	5.55
5IL2	484.7	31-1	16.68
5IL3	473.0	32-3	8.53
5IL4	469.8	31-2	14.49
5IL5	553.8	32-2	4.45
5IL6	547.4	31-3	11.08
5IL7 }	-	32-1	5.45
5IL7 }		31-4	15.64
5CL1	-	26-4	3.51
5CL2	447.9	25-1	20.13
5CL3	610.2	26-3	4.01
5CL4	556.1	25-2	17.53
5CL5	495.4	26-2	3.20
5CL6	554.7	25-3	16.52
5CL7 }	-	26-1	5.39
5CL7 }		25-4	18.56

^{238}U Foil Samples		^{238}U Track Recorder Samples	
Sample No.	Weight, mg	Sample No.	Weight, ng
8RL1	-	34-3	not determined
8RL2	1143.0	33-3	"
8RL3	1027.8	34-2	"
8RL4	809.9	33-2	"
8IL1	-	27-2	79.0
8IL2	1217.7	28-3	360.0
8IL3	1208.8	27-3	79.8
8IL4	1025.9	28-2	326.1
8CL1	-	21-2	74.75
8CL2	1273.4	22-2	157.0
8CL3	1050.2	21-3	90.78
8CL4	861.2	22-3	174.0

TABLE V. Weights of ^{239}Pu Samples in the Fission-yield Packets

Foil Samples		Track Recorder Samples	
Sample No.	Weight, mg	Sample No.	Weight, mg
9RL1	-	35-4	46.98
9RL2	550	36-1	3.86
9RL3	620	35-3	55.93
9RL4	632	36-2	9.04
9RL5	530	35-2	43.20
9RL6	659	36-3	9.42
9RL7 }	-	36-4	13.69
9RL7 }		35-1	59.73
9IL1	-	29-4	56.72
9IL2	502	30-1	9.04
9IL3	626	29-3	55.23
9IL4	609	30-2	7.32
9IL5	512	29-2	63.88
9IL6	528	30-3	7.51
9IL7 }	-	30-1	10.18
9IL7 }		29-1	62.02
9CL1	-	23-4	45.25
9CL2	543	24-1	2.60
9CL3	557	23-3	50.76
9CL4	474	24-2	10.81
9CL5	485	23-2	56.26
9CL6	637	24-3	3.04
9CL7 }	-	24-4	12.42
9CL7 }		23-1	45.16

TABLE VI. Weights of ^{242}Pu and ^{237}Np Samples in Fission-yield Packets

^{242}Pu Foil Samples		^{242}Pu Track Recorder Samples	
Sample No.	Weight, mg	Sample No.	Weight, ng
2CL	74.5	21-4	32
2CL	74.5	22-1	91
2IL	139.4	27-4	42
2IL	139.4	28-1	110
None	-	34-1	277
None	-	33-1	110
^{237}Np Foil Samples		^{237}Np Track Recorder Samples	
Sample No.	Weight, mg	Sample No.	Weight, ng
7CL	401.9	21-1	40.3
7CL	401.9	22-1	67.9
7IL	447.3	27-1	48.5
7IL	447.3	28-4	114.0
7RL	531.3	33-4	115.0
7RL	531.3	34-4	572.0

TABLE VII. Weights of ^{235}U and ^{238}U Samples in the Dosimetry Packets

^{235}U		^{238}U	
Sample No.	Wt., mg	Sample No.	Wt., mg
5R-1	1343.1	8R-1	2065.5
-2	1339.5	-2	2176.7
-3	2741.2	-3	4273.2
-4	1748.4	-4	2665.5
5I-1	430.2	8I-1	586.5
-2	452.8	-2	695.1
-3	1192.9	-3	1797.5
-4	1567.3	-4	2644.5
-5	1595.1	-5	2669.7
-6	468.4	-6	905.2
-7	485.7	-7	698.1
-8	958.6	-8	1609.8
5C-1	428.6	8C-1	732.5
-2	449.9	-2	743.9
-3	1168.7	-3	1990.0
-4	1554.6	-4	2614.6
-5	1603.0	-5	2625.1
-6	453.8	-6	729.4
-7	457.0	-7	740.0
-8	991.0	-8	1526.8

TABLE VIII. Weights of Ni and Al Samples in the Dosimetry Packets

Nickel						Aluminum	
Sample No.	Wt., mg	Sample No.	Wt., mg	Sample No.	Wt., mg	Sample No.	Wt., mg
NR-1	362.4	NI-17	115.6	NC-21	106.0	1AC-1	33.5
-2	356.2	-18	271.3	-22	116.7	-2	35.8
-3	709.9	NI-21	110.9	-23	306.3	-3	95.1
-4	457.5	-22	113.5	-24	412.1	-4	127.4
NR-11	351.1	-23	309.0	-25	422.3	-5	129.6
-12	353.4	-24	412.1	-26	120.2	-6	37.4
-13	685.9	-25	417.4	-27	120.6	-7	36.9
-14	440.4	-26	118.1	-28	279.5	-8	88.0
NR-21	357.6	-27	119.1			1AC-11	31.3
-22	347.3	-28	277.9			-12	35.9
-23	698.4	NC-1	109.4			-13	88.3
-24	445.5	-2	113.0			-14	118.5
NI-1	102.3	-3	306.2			-15	120.3
-2	116.9	-4	409.1			-16	34.2
-3	309.1	-5	425.3			-17	34.3
-4	410.7	-6	120.1			-18	82.4
-5	419.5	-7	125.0			1AC-21	32.5
-6	118.5	-8	275.7			-22	34.4
-7	117.9	NC-11	104.9			-23	97.0
-8	279.9	-12	112.8			-24	128.7
NI-11	106.8	-13	297.2			-25	130.4
-12	116.7	-14	399.1			-26	37.4
-13	300.4	-15	403.3			-27	36.4
-14	398.5	-16	116.0			-28	87.9
-15	404.5	-17	116.1				
-16	114.9	-18	269.8				

TABLE IX. Weights of Au Samples in the Dosimetry Packets

Gold					
Sample No.	Wt., mg	Sample No.	Wt., mg	Sample No.	Wt., mg
1GR-1	16.1	3GR-11	15.7	3GI-5	52.1
-2	15.1	-12	16.0	-6	13.5
-3	29.8	-13	28.9	-7	15.5
-4	18.0	-14	18.9	-8	29.7
1GR-11	16.0	3GR-21	15.7	1GC-1	5.6
-12	14.8	-22	14.8	-2	5.0
-13	29.4	-23	29.6	-3	12.5
-14	18.2	-24	18.6	-4	17.7
1GR-21	15.5	1GI-1	16.4	-5	18.4
-22	14.0	-2	14.8	-6	4.6
-23	29.9	-3	39.4	-7	4.9
-24	18.3	-4	54.3	-8	12.3
2GR-1	16.2	-5	56.6	1GC-11	5.1
-2	16.0	-6	14.5	-12	4.6
-3	28.2	-7	16.6	-13	12.1
-4	18.9	-8	33.4	-14	17.3
2GR-11	16.7	2GI-1	15.2	-15	17.3
-12	15.8	-2	12.8	-16	4.7
-13	28.8	-3	35.3	-17	4.6
-14	18.8	-4	49.3	-18	11.9
2GR-21	15.9	-5	52.0	1GC-21	5.7
-22	15.2	-6	13.5	-22	5.0
-23	27.8	-7	15.6	-23	12.6
-24	18.9	-8	30.4	-24	17.3
3GR-1	15.5	3GI-1	15.8	-25	18.8
-2	15.5	-2	14.1	-26	4.4
-3	28.1	-3	35.7	-27	4.9
-4	18.9	-4	49.5	-28	12.2

reduced by several percent the uncertainty associated with determining sample thickness and self-absorption. The overall uncertainty introduced into the final results owing to geometry corrections was in all cases less than ±1%.

IV. IMPROVEMENTS IN THE ACTIVATION-RATE MEASUREMENTS IN THE ZPR-3 MOCKUP CRITICAL EXPERIMENTS INCORPORATED AFTER ASSEMBLY 60

The ZPR-3 mockup critical experiments, Assemblies 60-63, took place over a period of nine months. Measurements and analysis of the activation-rate data for the four assemblies spanned a period of about 1.5 years. During this time, it was possible to incorporate several improvements that resulted in significant increases in the accuracies of the measured absolute reaction rates. Two important improvements in the accuracy of the Assembly 61 experiments resulted from the following: (1) the improved accuracy of the detector efficiency calibrations which was made possible by the availability of much improved absolute gamma-ray standards, and (2) the use of more accurate fission yields for the fission products measured in the Assembly 61 experiment; these fission yields, which were obtained in the Assembly 60 and 61 experiments, were more accurate than those which had been available previously.

The results of the Assembly 60 experiment, Ref. 1, were published before either of these improvements were possible. Also, results from all four assemblies (60-63) were reported in the Reactor Development Program Progress Reports as the data became available, and again the data were published before it was possible to incorporate these improvements. However, to provide the most accurate data possible, we have chosen to reflect these improvements in the data presented in this report on Assembly 61 and in the forthcoming report on Assemblies 62 and 63. Thus, the reaction-rate data previously issued in the report on Assembly 60[6] may not appear to be completely consistent with the later reports. However, Appendix A of the present report summarizes the changes in the Assembly 60 data to reflect the improvements. Because these changes only affect the absolute magnitudes of the reaction rates and do not affect the relative rates for a given Assembly, we expect that these changes will have a minimal effect upon the usefulness of the overall EBR-II mockup activation-rate data. It should be noted, however, that the results for Assemblies 60-63 are documented in the Reactor Development Program Progress Reports without the improvements. These results appear in Ref. 6 for Assembly 60, Ref. 7 for Assembly 62, and Ref. 8 for Assembly 63.

A. Detector Efficiency Calibrations

At the initiation of the EBR-II mockup critical experiments, as has been described in Ref. 1, the detector calibrations were made using five absolute gamma-ray standards and ^{152}Eu as a relative standard. During the course of these mockup experiments, we obtained a set of seven absolute standards from IAEA and a $^{140}Ba/^{140}La$ absolute standard from Amersham/Searle. These new standards enabled us to extend the range of the absolute calibration curve from 1.33 MeV to 1.84 MeV, revealed a 6% change in the

low energy region of the curve due to a change in efficiency for ^{57}Co, and provided valuable absolute calibration points between 0.136 and 0.511 MeV which had previously required interpolation. Since our data processing code requires a polynomial function of ln efficiency vs. ln energy, these new gamma standards allowed us to determine the efficiency polynomial for each detector with much greater accuracy. The overall effect was a 6% change at low energy (0.122-0.136 MeV), zero change at 0.662 MeV and a change of about 5% above 1.33 MeV. For all nuclides, except ^{237}Np, measured in the mockup critical experiments, these changes were within our previously assigned absolute errors. The most recent standards, however, allow us to reduce the uncertainty in efficiency calibrations to between 1.5-3% over the energy region required for these experiments. A complete description of the new detector calibration methods is presented in Ref. 10.

B. Absolute Fission Yields

To determine a fission rate from activation-rate data, one must apply a fission yield. Reference 1 stated that at the time the cited report was written, the fast-neutron fission yields for ^{235}U, ^{238}U, and ^{239}Pu were not well known. In an attempt to minimize the problem arising from inadequately known fission yields, a self-consistent set of fission yields based upon Meek and Rider's compilation[11] was used. An important aspect of the EBR-II mockup critical experiments was the opportunity to measure several of these fission-product yields in a typical fast breeder reactor spectrum. From the Assembly 60 and 61 irradiations of the Y-foils, more accurate yields have been determined. The raw data from which the yields were determined are presented in Ref. 1 and in this report; however, a complete description of the yield determinations and their accuracies will be the subject of a subsequent report. A preliminary discussion of these measurements and results of the fast-neutron fission-yield studies is presented in Ref. 10. Table X has been used for the determination of the fission rates presented in this report and will be used in the subsequent report describing Assemblies 62 and 63. It is important to recognize that the new yields were not used in the Assembly 60 report, simply because the data were not available; therefore, comparisons of absolute fission rates between those in Ref. 1 and those in succeeding reports of the EBR-II mockup experiments will have a built-in bias.

V. RESULTS

The absolute reaction rates have been computed from the following equation:

$$(\sigma\phi) = \frac{\lambda N_o}{n(1 - e^{-\lambda t})}$$

TABLE X. Fission Product Yield Information Obtained from the Mockup Critical Experiments

Reaction	Fission Product	Measured Yields[a], %	Inferred Yields[b], %	Meek & Rider Yields[c], %
$^{235}U(n,f)$	^{95}Zr	6.41	6.7	6.7
	^{97}Zr	5.53	6.3	6.8
	^{140}Ba	5.67	5.9	5.6
	^{132}Te	4.77	4.5	5.5
	^{143}Ce	-	5.3	5.4
	^{131}I	3.44	3.3	3.7
	^{103}Ru	3.29	3.3	3.5
$^{238}U(n,f)$	^{95}Zr	5.44	5.7	5.8
	^{97}Zr	5.91	6.1	4.9
	^{140}Ba	5.92	6.1	6.0
	^{132}Te	5.36	5.3	4.4
	^{143}Ce	-	4.0	4.3
	^{131}I	3.66	3.4	3.2
	^{103}Ru	6.29	6.2	5.8
$^{239}Pu(n,f)$	^{95}Zr	4.77		
	^{97}Zr	4.86		
	^{140}Ba	5.25		
	^{132}Te	5.36		
	^{143}Ce	-		
	^{131}I	4.77		
	^{103}Ru	7.05		
$^{237}Np(n,f)$	^{140}Ba	5.41		
$^{242}Pu(n,f)$	^{140}Ba	4.95		

[a] Measured in Mockup Critical Experiments, Ref. 10

[b] Values used for Assembly 60, Ref. 1.

[c] Recommended fission-yield values from M. E. Meek, and B. F. Rider, Ref. 11.

where N_o is the measured number of reaction-product atoms present at the end of the irradiation, λ is the decay constant for the reaction product expressed in units of sec^{-1}, n is the number of target atoms irradiated in the sample, and t is the time of the irradiation. The quantity $(\bar{\sigma}\phi)$ is often referred to as the saturated activity, and is expressed in units of atoms of reaction product per target atom-second.

A. Results from the Dosimetry Packets

Tables XI and XII summarize the results of the $^{197}Au(n,\gamma)^{198}Au$ and $^{58}Ni(n,p)^{58}Co$ reaction rates, respectively. Table XIII tabulates the $^{27}Al(n,\alpha)^{24}Na$ and $^{238}U(n,\gamma)^{239}U$ results. Table XIV summarizes the $^{235}U(n,f)$ and $^{238}U(n,f)$ fission-rate results. The sample numbers in these tables may be correlated with their respective irradiation locations within a foil packet by referring to Fig. 8. The absolute errors for the reaction-rate measurements are as follows: $^{197}Au(n,\gamma)$, 8.1%; $^{58}Ni(n,p)$, 5.9%; $^{27}Al(n,\alpha)$, 7.1-7.6%; and $^{238}U(n,\gamma)$, 6.1-7.5%. The absolute errors of the fission-rate results are of the order of ±6%. Tables XV and XVI summarize the production rates of seven fission products determined from the ^{235}U and ^{238}U dosimetry samples, respectively. The errors quoted in Tables XV and XVI are the total absolute uncertainties in each measurement.

The fission-rate results from the fission-yield packets are tabulated in Table XVII for ^{235}U, Table XVIII for ^{239}Pu, and Table XIX for ^{238}U, ^{242}Pu, and ^{237}Np. These tables include the fission rates determined by measurements of the massive foils and the use of the fission yields given in Table X, and by direct measurement of the fissions registered in the solid-state track recorders. Fission rates are given for only a few of the massive foils since some were dissolved for radiochemical analysis and others, which were counted solely to confirm results, are not given. The foils for which rates are given were generally counted over 10 times for the various fission products. The absolute error of the fission rates obtained with the massive foils is about ±7%, and the uncertainty in the track-recorder results is about ±1.5%, except for ^{238}U and ^{242}Pu, which have an uncertainty of about ±2.5%.

The absolute reaction rates measured in the dosimetry packets and in the massive fission-yield foils are plotted in Fig. 9 as a function of position within each drawer location. The fission-yield foils were irradiated in vertical strips relative to the drawer plate composition, and the dashed lines in Fig. 9 showing these results are averages of the several individual measurements. The Y-foil data are plotted in Fig. 9 so as to be comparable to the D-foil data, with the understanding that the flux gradient across the drawers on the right side of the assembly (Y packets) is a mirror image of the gradient across the left side (D packets). The abscissa in Fig. 9 is given in terms of line length, which corresponds approximately to the width of each sample in units of 1/32 of an inch; the ordinate is the absolute reaction rate. This plot of the D data emphasizes the flux gradients within a drawer and illustrates the heterogeneity within a given drawer location.

The comparison of data for the D and Y foil sets, as shown in Fig. 9, emphasizes the detailed heterogeneity effects within a given drawer location. A more general comparison of data can be made by comparing drawer-

TABLE XI. Absolute $^{197}Au(n,\gamma)^{198}Au$ Reaction Rates in ZPR-3 Assembly 61 Dosimetry Packets

Sample	Absolute Reaction Rate x 10^{16}, sec^{-1}	Relative Error, %		Absolute Reaction Rate x 10^{16}, sec^{-1}	Relative Error, %		Absolute Reaction Rate x 10^{16}, sec^{-1}	Relative Error, %
1R-1	689	0.10	2R-1	625	0.15	3R-1	721	0.84
2	670	0.31	2	600	0.35	2	695	0.19
3	673	0.53	3	607	0.28	3	696	0.47
4	640	0.72	4	579	0.35	4	653	0.40
11	680	0.24	11	609	0.24	11	697	0.27
12	644	1.1	12	580	0.34	12	654	0.17
13	651	0.43	13	586	0.10	13	670	0.30
14	611	0.30	14	548	0.24	14	633	0.46
21	733	0.21	21	626	0.79	21	725	0.10
22	672	0.67	22	620	0.43	22	689	0.21
23	672	0.53	23	609	0.29	23	695	0.25
24	635	0.22	24	571	0.33	24	654	0.29
1I-1	181	0.10	2I-1	175	0.28	3I-1	190	0.82
2	168	0.25	2	160	0.10	2	173	0.29
3	129	0.38	3	123	0.40	3	129	1.34
4	106	0.35	4	104	0.64	4	107	0.24
5	95.3	0.71	5	94.4	0.25	5	96.4	0.23
6	91.0	0.22	6	88.5	0.55	6	88.9	0.44
7	85.7	0.54	7	82.5	0.80	7	85.7	0.45
8	85.2	0.76	8	84.2	1.0	8	85.9	0.16
C-1	82.5	0.35	C-11	86.3	0.40	C-21	86.2	0.70
2	86.1	1.02	12	86.8	0.40	22	85.2	0.23
3	83.7	0.19	13	83.2	0.10	23	84.3	0.16
4	86.2	0.29	14	86.2	0.34	24	86.6	0.29
5	86.2	0.56	15	86.4	0.44	25	86.0	0.20
6	86.0	0.52	16	84.4	0.33	26	86.4	0.10
7	85.0	0.45	17	85.9	0.84	27	85.2	0.53
8	85.7	0.36	18	85.7	0.54	28	86.7	0.81

TABLE XII. Absolute $^{58}Ni(n,p)^{58}Co$ Reaction Rates in ZPR-3 Assembly 61 Dosimetry Packets

Sample	Absolute Reaction Rate x 10^{16}, sec^{-1}	Relative Error, %	Sample	Absolute Reaction Rate x 10^{16}, sec^{-1}	Relative Error, %
Reflector			Interface		
1	0.553	0.70	23	5.45	0.62
2	0.688	0.10	24	5.63	0.10
3	0.821	0.60	25	6.18	0.15
4	1.014	0.15	26	6.76	0.10
11	0.587	1.4	27	7.07	0.71
12	0.717	0.83	28	6.77	0.63
13	0.863	1.0	Core	9.88	0.65
14	1.061	0.30	1	9.99	0.22
21	0.571	0.86	2	10.38	1.1
22	0.711	0.85	3	10.05	0.31
23	0.864	0.46	4	10.31	0.42
24	1.049	0.30	5	10.75	0.43
Interface					
1	4.53	0.53	6	10.86	0.28
2	4.58	0.10	7	10.34	0.10
3	5.28	0.13	8	10.14	0.23
4	5.45	0.10	11	10.16	1.7
5	5.60	0.58	12	10.75	0.14
6	6.57	0.94	13	10.26	0.10
7	6.93	0.26	14	10.45	0.21
8	6.56	0.11	15	10.97	0.14
11	4.50	0.36	16	10.97	0.78
12	4.73	0.95	17	10.62	0.13
13	5.46	0.73	18	10.06	0.46
14	5.61	0.10	21	10.24	0.59
15	6.21	0.49	22	10.43	0.10
16	6.73	0.32	23	10.21	0.13
17	7.14	0.17	24	10.45	0.29
18	6.78	0.10	25	10.97	0.10
21	4.52	0.42	26	11.18	0.57
22	4.72	1.2	27	10.46	0.10
			28		

TABLE XIII. Absolute $^{27}Al(n,\alpha)^{24}Na$ and $^{238}U(n,\gamma)^{239}U$ Reaction Rates in ZPR-3 Assembly 61 Dosimetry Packets

$^{27}Al(n,\alpha)^{24}Na$			$^{238}U(n,\gamma)^{239}U$		
Sample	Absolute Reaction Rate x 10^{14}, sec^{-1}	Relative Error, %	Sample	Absolute Reaction Rate x 10^{15}, sec^{-1}	Relative Error, %
Core			Blanket		
1	6.32	0.73	1	10.5	2.2
2	6.24	1.3	2	10.4	1.5
3	6.64	0.33	3	9.5	0.85
4	6.24	1.3	4	10.2	0.87
5	6.47	1.0	Interface		
6	6.69	0.41	1	5.83	1.3
7	6.98	1.4	2	5.46	1.6
8	6.51	0.75	3	4.50	2.5
11	6.37	1.0	4	4.05	1.4
12	6.36	1.0	5	4.02	1.6
13	6.94	1.1	6	3.93	2.3
14	6.72	2.3	7	4.14	1.8
15	6.68	2.9	8	4.24	1.5
16	6.85	0.68	Core		
17	7.23	0.73	1	5.04	0.95
18	6.65	0.75	2	4.96	1.3
21	6.41	2.9	3	4.82	2.4
22	6.50	1.1	4	4.79	2.7
23	6.77	1.6	5	5.06	1.5
24	6.53	0.27	6	5.09	1.1
25	6.56	0.68	7	5.18	1.2
26	6.93	0.99	8	5.27	1.9
27	7.04	2.1			
28	6.64	0.67			

TABLE XIV. Absolute Fission Rates of ^{235}U and ^{238}U in ZPR-3 Assembly 61 Dosimetry Packets

Sample Location		Absolute Fission Rate [10^{-15} fissions/(atom)(sec)] ^{235}U Rate	^{235}U Relative Error, %	^{238}U Rate	^{238}U Relative Error, %
Reflector	1	50.0	1.8	0.257	1.9
	2	50.3	1.9	0.304	1.9
	3	50.4	1.8	0.364	2.0
	4	52.9	2.0	0.435	2.3
	Ave	50.9		0.356	
Interface	1	43.2	2.0	1.66	2.2
	2	43.3	2.0	1.75	2.0
	3	39.8	2.2	1.89	1.8
	4	39.3	2.0	1.92	2.1
	5	39.4	2.0	2.16	1.9
	6	41.3	1.8	2.36	2.3
	7	41.3	2.2	2.47	1.9
	8	41.2	2.0	2.35	1.9
	Ave	40.5		2.08	
Core	1	49.4	2.0	3.27	2.1
	2	49.4	1.7	3.31	2.0
	3	49.7	1.9	3.32	1.9
	4	50.3	1.9	3.17	2.0
	5	49.5	1.9	3.28	1.8
	6	50.7	1.7	3.47	1.8
	7	52.7	2.0	3.40	1.9
	8	50.6	1.9	3.37	1.9
	Ave	50.1		3.31	

TABLE XV. ^{235}U Absolute Fission Product Rates From Dosimetry Packets
[10^{-15} atoms/(atom ^{235}U)(sec)]

Sample		^{97}Zr		^{103}Ru		^{140}Ba		^{132}Te		^{131}I		^{143}Ce		^{95}Zr	
		Rate	Error, %	Rate	Error, %	Rate	Error, %	Rate	Error, %	Rate	Error, %	Rate	Error, %	Rate	Error, %
Reflector	1	3.02	4.2	1.58	4.9	3.03	3.7	2.33	6.1	1.48	4.3	2.34	5.5	3.36	4.4
	2	3.05	3.7	1.59	6.0	3.03	3.5	2.37	6.6	1.61	4.5	2.26	5.9	3.34	4.3
	3	2.99	3.8	1.68	5.1	3.11	3.7	2.52	6.0	1.43	4.3	2.17	6.1	3.42	4.1
	4	3.22	4.3	1.62	5.7	3.08	3.6	2.90	7.9	1.48	4.5	2.41	5.4	3.44	4.0
Interface	1	2.65	4.6	1.39	3.6	2.55	4.4	2.00	6.2	1.24	4.5	1.91	3.7	3.06	5.9
	2	2.55	3.7	1.43	3.6	2.60	4.7	2.02	6.5	1.28	3.9	1.85	4.2	3.11	6.1
	3	2.33	5.1	1.24	4.7	2.37	4.5	1.93	6.6	1.19	3.9	1.81	5.7	2.80	6.2
	4	2.33	4.2	1.24	4.7	2.37	4.4	1.92	6.6	1.18	4.0	1.66	4.5	2.78	5.8
	5	2.27	3.9	1.31	4.2	2.34	4.5	1.87	6.5	1.18	5.0	1.70	4.5	2.84	5.5
	6	2.48	3.3	1.38	3.4	2.45	4.5	1.97	6.4	1.19	3.5	1.85	3.3	2.86	5.6
	7	2.68	7.3	1.40	4.0	2.45	4.5	1.99	6.3	1.26	3.6	1.84	4.2	2.91	5.6
	8	2.36	4.3	1.45	3.6	2.43	4.6	2.01	6.6	1.28	3.4	1.76	3.7	2.85	6.1
Core	1	2.93	6.5	1.56	4.6	2.91	3.5	2.39	6.0	1.60	4.4	2.23	4.6	3.35	4.4
	2	2.95	3.8	1.60	5.3	2.89	3.6	2.43	6.2	1.59	3.9	2.19	4.5	3.30	4.0
	3	2.95	3.5	1.41	4.5	2.86	3.5	2.52	6.6	1.61	4.6	2.38	5.0	3.29	5.0
	4	3.06	3.5	1.49	5.1	2.92	4.1	2.46	6.6	1.62	4.2	2.34	5.5	3.36	5.1
	5	3.03	3.6	1.64	5.6	2.92	3.6	2.29	6.0	1.55	5.6	2.19	5.3	3.37	4.9
	6	3.09	3.6	1.66	4.5	2.93	4.0	2.45	6.1	1.65	4.5	2.29	4.7	3.33	4.0
	7	3.07	3.7	1.72	4.5	3.02	3.6	2.74	6.0	1.69	4.2	2.37	5.0	3.45	6.3
	8	3.06	4.3	1.63	4.5	2.91	3.6	2.44	6.7	1.61	4.0	2.38	6.1	3.34	4.2

TABLE XVI. ^{238}U Absolute Fission Product Rates From Dosimetry Packets
[10^{-16} atoms/(atom ^{238}U)(sec)]

Sample		^{97}Zr		^{103}Ru		^{140}Ba		^{132}Te		^{131}I		^{143}Ce		^{95}Zr	
		Rate	Error, %	Rate	Error, %	Rate	Error, %	Rate	Error, %	Rate	Error, %	Rate	Error, %	Rate	Error, %
Reflector	1	0.163	3.7	0.173	5.1	0.160	3.7	0.157	6.1	0.084	4.7	0.084	5.3	0.118	5.8
	2	0.190	3.9	0.190	5.4	0.191	3.8	0.180	6.2	0.098	5.1	0.084	5.3	0.179	4.7
	3	0.219	3.6	0.231	4.8	0.218	3.7	0.196	6.1	0.115	6.3	-	-	0.207	4.5
	4	0.275	3.7	0.293	4.7	0.276	3.6	0.254	6.2	0.146	4.9	0.123	13.5	0.225	8.6
Interface	1	1.02	3.4	1.09	3.9	1.07	4.7	0.926	6.7	0.456	8.4	0.556	4.5	0.952	8.4
	2	1.03	3.5	1.11	3.9	1.11	4.8	0.941	6.2	0.545	5.9	0.575	6.3	1.09	6.4
	3	1.16	3.4	1.27	3.5	1.20	4.6	1.04	6.5	0.540	5.7	0.562	4.1	1.14	5.4
	4	1.22	3.7	1.22	4.6	1.23	5.0	1.04	6.5	0.516	4.0	0.592	5.0	1.22	7.2
	5	1.33	3.5	1.39	3.5	1.36	4.5	1.20	7.3	0.626	3.6	0.744	3.8	1.27	5.8
	6	1.50	4.6	1.48	4.7	1.49	4.6	1.26	6.7	0.612	6.7	0.795	4.6	1.53	7.8
	7	1.44	4.4	1.61	3.8	1.54	4.5	1.39	6.3	0.754	4.1	0.831	3.9	1.45	5.4
	8	1.48	3.5	1.46	4.7	1.48	4.7	1.29	6.7	0.704	3.5	0.860	3.8	1.34	5.8
Core	1	1.89	3.6	2.00	6.0	1.97	3.5	1.81	6.1	1.10	4.0	1.36	4.7	1.84	7.7
	2	1.98	3.6	1.99	6.8	2.00	3.5	1.75	6.0	1.04	4.1	1.36	5.2	2.00	5.4
	3	1.94	4.1	2.14	5.1	2.01	4.1	1.82	6.3	1.05	4.7	1.32	4.7	1.85	4.9
	4	1.81	3.8	1.78	7.1	1.95	4.0	1.79	6.4	1.04	4.4	1.30	5.5	1.92	4.9
	5	1.95	3.8	2.05	4.8	1.99	3.6	1.84	6.3	1.02	5.4	1.29	4.8	1.88	4.3
	6	2.08	3.7	2.12	4.7	2.09	4.2	1.94	6.3	1.11	4.0	1.45	4.8	1.91	4.3
	7	2.05	3.5	2.10	4.9	2.05	4.2	1.90	6.2	1.10	4.7	1.36	4.7	1.90	6.1
	8	2.04	4.6	2.14	5.3	2.03	4.0	1.87	6.0	1.05	4.5	1.38	5.0	1.81	4.9

TABLE XVII. Absolute Fission Rates of ^{235}U in ZPR-3 Assembly 61 Fission Yield Packets

Sample Location	Absolute Fission Rate [10^{-15} fissions/(atom)(sec)]				
	Massive Foils		SSTR Foils		
	Sample Number	Fission Rate	Sample Number	Fissions/ nanogram	Fission Rate
Core	5CL-1	-	-		
	2	48.9	25-1	440	47.7
	3	-	26-3	473	51.3
	4	46.6	25-2	466	50.5
	5	-	26-2	424	46.0
	6	48.9	-		
	7	-	26-1	442	47.9
	7	-	25-4	451	48.9
Interface	5IL-1	-	32-4	355	38.5
	2	37.5	-		
	3	-	32-3	333	36.1
	4	36.6	-		
	5	-	32-2	350	37.9
	6	35.7	-		
	7	-	32-1	329	35.7
Reflector	1	-	37-4	493	53.4
	2	45.3			
	3	-	37-3	464	50.3
	4	44.5			
	5	-	37-2	481	52.1
	6	46.0			
	7	-	37-1	471	51.1

TABLE XVIII. Absolute Fission Rates of ^{239}Pu in ZPR-3 Assembly 61 Fission-yield Packets

Sample Location	Absolute Fission Rate [10^{-15} fissions/(atom)(sec)] Massive Foils Sample Number	Massive Foils Fission Rate	SSTR Foils Sample Number	SSTR Foils Fissions/ nanogram	SSTR Foils Fission Rate
Core	9CL-1	-	23-4	538	59.3
	2	60.3	24-1	-	-
	3	-	23-3	536	59.1
	4	61.0	24-2	511	56.3
	5	-	23-2	526	58.0
	6	58.0	24-3	-	-
	7	-	24-4	528	58.2
	7	-	23-4	538	59.3
Interface	9IL-1	-	29-4	362	39.9
	2	41.3	30-1	376	41.4
	3	-	29-3	379	41.8
	4	39.3	30-2	362	39.9
	5	-	29-2	352	38.8
	6	41.8	30-3	378	41.7
	7	-	30-4	381	42.0
	7	-	29-4	362	39.9
Reflector	9RL-1	-	35-4	516	56.9
	2	41.6	36-1	500	55.1
	3	-	35-3	497	54.8
	4	41.0	36-2	491	54.1
	5	-	35-2	481	53.0
	6	40.7	36-3	478	52.7
	7	-	36-4	510	56.2
	7	-	35-4	516	56.9

TABLE XIX. Absolute Fission Rates of ^{238}U, ^{242}Pu, and ^{237}Np in ZPR-3 Assembly 61 Fission-yield Packets

		Absolute Fission Rate [10^{-15} fissions/(atom)(sec)]				
		Massive Foils		SSTR Foils		
Fissile Material	Sample Location	Sample Number	Fission Rate	Sample Number	Fissions/ nanogram	Fission Rate
^{238}U	Core	8CL-1	-	21-2	28.9	3.17
		2	3.24	22-2	27.8	3.05
		3	3.18	21-3	29.9	3.28
		4	-	22-3	29.1	3.20
	Interface	8IL-1	-	27-2	18.1	1.99
		2	2.32	28-2	18.5	2.03
		3	2.31	27-3	23.5	2.58
		4	-	28-3	18.4	2.02
	Reflector	8RL-2	0.495	-		
		3	0.496	-		
^{242}Pu	Core	2CL-1	-	21-4	180	20.1
		-		22-4	164	18.3
	Interface	2IL-1	-	27-4	107	11.9
		-		28-1	104	11.6
	Reflector	-		34-1	34.6	3.86
		-		33-1	35.7	3.98
^{237}Np	Core	7CL-1	18.0	21-1	194	21.2
		-		22-1	190	20.8
	Interface	7IL-1	11.5	27-1	130	14.2
		-		28-1	127	13.9
	Reflector	7RL-1	3.91	33-1	34.9	3.81
		-		34-1	42.3	4.62

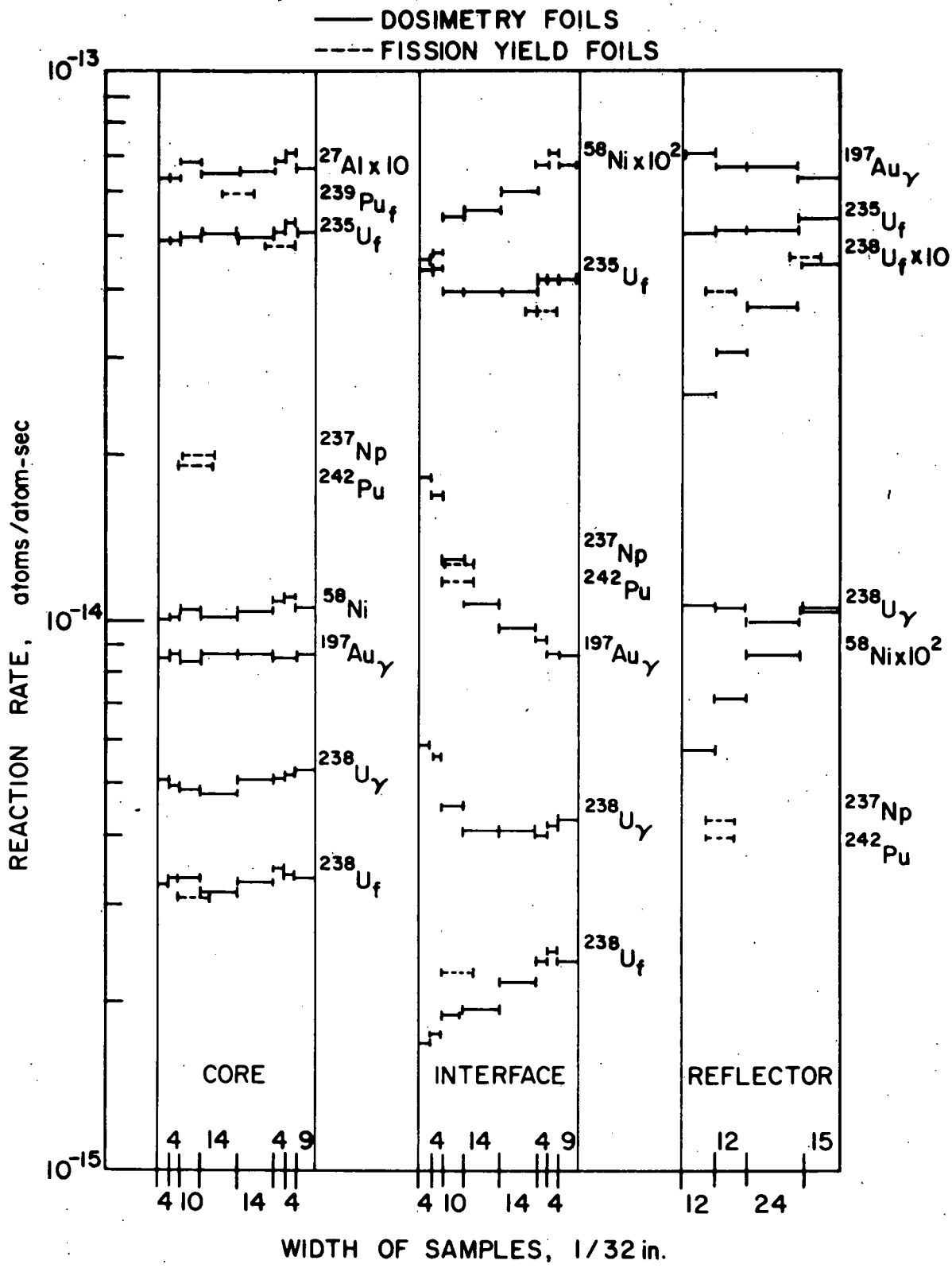

Fig. 9. Absolute Reaction Rates in the D and Y Foil Packets Irradiated in the Core, Interface, and Reflector Positions of Assembly 61

averaged reaction rates, which are obtained by averaging the individual measurements from each of the samples at a given drawer location. For the dosimetry sets this averaging must be weighted by the weight of each sample to achieve a true drawer average. A true drawer average cannot be obtained for the fission-yield or track-recorder measurements because the sample strips were irradiated parallel to the plate geometry of the drawer, as shown in Figs. 4-7. However, for purposes of comparison, we have averaged the individual samples in each strip and called it a drawer average. Maddison[5] has reported the results of his measurements (A foils) and it is of interest to compare his results, averaged over each drawer location, with the results reported here. His results are reported in units of $(\text{gram-hrs})^{-1}$; therefore, to make a valid comparison, it is necessary to convert his units into units of $(\text{sec})^{-1}$. In addition, his fission-rate values were determined by measuring only the fission product ^{97}Zr, and applying a fission-yield value of 5.77% for ^{235}U and a value of 5.99% for ^{238}U. To provide a consistent comparison, we have converted his results to reflect the fission rates based upon the ^{97}Zr fission yields measured in the Assemblies 60 and 61 tests which are given in Table X. The drawer-averaged fission and reaction rates, as measured in the D, Y, T (solid-state track recorders), and A foil sets, are tabulated in Table XX.

Finally, Table XXI summarizes a number of reaction-rate ratios as determined in the dosimetry samples. These ratios are, in fact, spectrum-averaged cross-section ratios, and are tabulated to show the sensitivity of the various ratios to the heterogeneity of the neutron flux across the core, interface, and reflector drawers. Also given in Table XXI are the drawer-averaged cross-section ratios as determined from the drawer-averaged reaction rates given in Table XX.

VI. DISCUSSION

An examination of the results shown in Fig. 9 and Table XX provides a means for evaluating the reproducibility and consistency of the various measurements. A direct comparison of the D and Y reaction rates is complicated because the orientation of the Y foils was parallel to the plates, whereas the orientation of the D foils was perpendicular to the plates. The Y foils were orientated in this manner because the primary objective was to obtain fission-yield measurements under conditions which would minimize effects of heterogeneity on the foils, whereas the placement of the D foils was intended to maximize the effects of heterogeneity on the foils. If one notes that the Y foils of ^{238}U, ^{242}Pu, and ^{237}Np were parallel and adjacent to the ^{235}U fuel in the drawers, i.e., exposed to the hardest portion of the neutron spectrum within a drawer, then a comparison of the drawer-averaged values in Table XX is reasonable. In comparing the fission rates of ^{235}U in the D foils with those of ^{235}U in the Y foils, we see a 2% deviation in the core and $\sim$10% deviations in the interface and reflector regions. The most probable explanation for the interface and reflector discrepancies is neutron self-shielding in the Y packets. This point will be discussed in more detail later; however, it should be noted that the D and T values for the fission rates of ^{235}U are in excellent agreement for all three positions where little or no self-shielding can occur. A comparison of the D, Y, and T fission rates for ^{238}U shows

TABLE XX. Drawer-averaged Fission and Reaction Rates at the Core, Interface, and Reflector Positions for the Dosimetry, Fission-yield, Solid-state Track Recorder Packets

Reaction	Foil Packet	Reaction Rate, $[10^{-15}$ atoms/(atom)(sec)] Core	Interface	Reflector
$^{235}U(n,f)$	D	50.1	40.5	50.9
	Y	48.1	36.6	45.3
	T	49.3	37.0	51.5
	A[a,b]	56.8	40.3	59.9
$^{238}U(n,f)$	D	3.31	2.08	0.356
	Y	3.10	2.23	0.395
	T	3.19	2.13	-
	A[a,b]	3.51	1.95	0.297
$^{239}Pu(n,f)$	Y	59.8	40.8	41.0
	T	58.6	40.2	54.3
$^{237}Np(n,f)$	Y	19.7	12.6	4.26
	T	21.0	14.0	4.21
$^{242}Pu(n,f)$	T	19.2	11.7	3.92
$^{238}U(n,\gamma)$	D	4.98	4.31	10.1
	A[b]	5.48	4.36	16.5
$^{197}Au(n,\gamma)$	D	8.57	11.0	66.3
	A[b]	8.41	9.97	62.6
$^{58}Ni(n,p)$	D	1.04	0.585	0.0816
	A[b]	0.987	0.558	0.0524
$^{27}Al(n,\alpha)$	D	0.00662		
	A[b]	0.00578		

[a] Based upon fission yields described in text.

[b] Data taken from Ref. 5, and converted to above units.

TABLE XXI. Spectrum Averaged Cross Section Ratios From Dosimetry Foil Packets

Sample Location		$\frac{^{238}U(n,f)}{^{235}U(n,f)}$	$\frac{^{238}U(n,\gamma)}{^{235}U(n,f)}$	$\frac{^{197}Au(n,\gamma)}{^{235}U(n,f)}$[b]	$\frac{^{58}Ni(n,p)}{^{235}U(n,f)}$	$\frac{^{238}U(n,\gamma)}{^{238}U(n,f)}$	$\frac{^{197}Au(n,\gamma)}{^{58}Ni(n,p)}$[b]
Reflector 0-9	1	0.0051	0.210	1.40	0.00114	40.9	1230
	2	0.0060	0.207	1.32	0.00140	34.2	939
	3	0.0072	0.188	1.32	0.00168	26.1	784
	4	0.0082	0.193	1.19	0.00197	23.4	603
	Ave.[a]	0.0070	0.198	1.27	0.00160	28.2	793
Interface 0-11	1	0.0384	0.135	0.419	0.0105	3.51	40.0
	2	0.0404	0.126	0.388	0.0108	3.12	36.0
	3	0.0475	0.113	0.322	0.0136	2.38	23.7
	4	0.0489	0.103	0.270	0.0141	2.11	19.1
	5	0.0548	0.102	0.242	0.0152	1.86	15.9
	6	0.0571	0.095	0.220	0.0162	1.67	13.6
	7	0.0598	0.100	0.208	0.0171	1.68	12.2
	8	0.0570	0.103	0.207	0.0163	1.80	12.7
	Ave.[a]	0.0513	0.107	0.273	0.0144	2.08	18.9
Core 0-15	1	0.0662	0.102	0.172	0.0202	1.54	8.50
	2	0.0670	0.100	0.174	0.0204	1.50	8.51
	3	0.0668	0.097	0.168	0.0211	1.45	7.97
	4	0.0630	0.095	0.172	0.0203	1.51	8.46
	5	0.0663	0.102	0.174	0.0210	1.54	8.29
	6	0.0684	0.100	0.169	0.0215	1.47	7.85
	7	0.0645	0.098	0.162	0.0209	1.52	7.75
	8	0.0666	0.104	0.170	0.0208	1.56	8.19
	Ave.[a]	0.0660	0.099	0.171	0.0208	1.50	8.22

[a] Drawer averaged ratios (averaged on the basis of sample weight).

[b] Front gold foil only.

reasonable agreement. In the core, the D values are ~10% higher than the Y values, while the T values are intermediate. Similar spreads among the three are found at the interface and the reflector, but the Y rates are 10% larger than the D values. The most probable explanation for the deviations is that the Y foils were exposed to the hardest portion of the neutron spectrum within a drawer, while the D foils were exposed to a more representative drawer-averaged neutron spectrum.

A comparison of the A foil sets with those reported herein is not, in general, very satisfactory. In the Assembly 60 experiment, the D and A foils agreed to about ±5%, whereas in the Assembly 61 experiment, the agreement is about ±10%. These differences are outside the experimental uncertainties, particularly for values obtained for ^{235}U in the core and reflector, for $^{238}U(n,f)$ in the reflector, for $^{238}U(n,\gamma)$ in the core and reflector, and for ^{58}Ni in the reflector. The unusual observation from this comparison is the relatively good agreement between A and D values for the interface position, and the generally poor agreement between the A and D values for the core and reflector positions.

Because of the very degraded neutron spectrum at the reflector position in Assembly 61 as compared with that in Assembly 60, we were concerned about the effects of neutron self-absorption in both the 0.2-mil gold foils and the 32-mil ^{235}U and ^{239}Pu foils in the fission-yield packets. The self-absorption effects are dominant for neutrons in the epithermal neutron region, and though there are relatively few neutrons in the low energy region (<1 keV), these along with the epithermal neutrons can contribute a significant fraction of the reaction rate. For example, gold has a 37,000 barn resonance at 4.9 eV; ^{235}U has fission resonances which exceed 500 barns at 8.8, 19.3, and 35.4 eV; and ^{239}Pu has fission resonances which exceed 500 barns at 8.0, 10.2, and 14.7 eV. All of these resonances and others may contribute an appreciable fraction of the measured reaction rate in a very degraded neutron spectrum; consequently, this effect may have resulted in resonance self-shielding for the Assembly 61 reflector measurements.

Without a detailed knowledge of the neutron-energy spectra below 1 keV, it is impossible to calculate the self-shielding effects in our samples. However, a 29-energy-group, diffusion-theory calculation has been made,[12] which provides an estimate of the neutron energies averaged over the three irradiation positions of Assembly 61. These estimates are in keV:

	Core	Interface	Reflector
Median Neutron Energy	442	402	175
Median ^{235}U Fission Energy	368	293	0.369
Average ^{235}U Fission Energy	765	670	110

For comparison, the median ^{235}U fission energy for the blanket position of Assembly 60 was calculated to be 132 keV. It must be recognized that these calculated energies at the interface and reflector positions are very sensitive to the distance from the core. The energies can also vary over the two-inch dimensions of a foil packet, and for this reason, these calculated neutron energies must be considered as nominal estimates.

To examine the effects of neutron self-shielding in gold, we irradiated three 0.2-mil-thick gold foils at both the interface and reflector positions of Assembly 61. The activation-rate results are tabulated in Table XI. The relative activation rates in the front, middle, and back gold foils averaged over the drawer position are 1.00, 0.89, and 1.03, respectively, for the reflector position and 1.00, 0.97, 1.02, respectively, for the interface position. Thus we find that the activation rate in the middle gold foil is reduced by about 11% in the reflector packet and by about 3% in the interface packet. The surprising observation is that the activation rate in the back foil (farthest from core center) is larger than that in the front foil by 3% in the reflector, and by 1.5% in the interface position. This effect may indicate a reverse-gradient of very low energy neutrons which are backscattered from the nickel reflector.

Stanford and Seckinger[13] have examined the problem of thickness corrections for neutron-activated gold foils in thermal and epithermal neutron environments. On the basis of this work, we would estimate that a 0.2-mil-thick gold foil will have a 30% reduction in activation rate if all the neutrons are epithermal. Since our observed activation rates for the center gold foil at the reflector and interface positions were low by ∿10% and ∿3% relative to the outside foils, we conclude that ∿30% of the neutrons are epithermal at the reflector and ∿10% are epithermal at the interface. Also, we calculate that the intensity of a 4.9 eV neutron beam will be degraded to 1/3 of its initial value in traversing a 0.2-mil-thick gold foil. If we assume that the gold activations due to epithermal neutrons are predominantly caused by the 4.9 eV resonance, then the middle gold foil will be reduced in activations by 1/9 relative to the front or back gold foil. We, therefore, can qualitatively account for the reduced activation in the middle gold foil. Furthermore, we estimate that the drawer-averaged reaction rate given in Table XX for $^{197}Au(n,\gamma)$ in the reflector position is low by about 10% owing to resonance self shielding, and that the interface value is low by about 3%.

The problem of neutron self-shielding also arises in the evaluation of the ^{235}U and ^{239}Pu foils, particularly those in the fission-yield packets which were 32 mils thick. Although this effect was negligible in the uranium blanket position in Assembly 60, it must be taken into account when considering the nickel reflector position in Assembly 61, since the neutron energy in this region was considerably lower than that in a comparable region in the uranium blanket. The magnitude of the self-shielding effect may be examined by comparing the fission rate as determined in the massive ^{235}U or ^{239}Pu samples with the rate for the same nuclide as measured by the "infinitely-thin" track recorders. This comparison can be made using Table XVII for ^{235}U and Table XVIII for ^{239}Pu. Reaction rates of both nuclides are given in Table XX as drawer averages. We see that at the core and interface positions for both ^{235}U and ^{239}Pu, the Y:T fission-rate ratios are close to unity. In the reflector position, however, the Y:T ratio is 0.88 for ^{235}U and 0.75 for ^{239}Pu. If we attribute this difference as being entirely due to neutron self-shielding, we can empirically estimate the magnitude of the neutron self-shielding in the 6-mil ^{235}U dosimetry foil packet. The magnitude of neutron self-shielding in the ^{235}U dosimetry foil in the reflector position is estimated to be 3%. However,

corrections have not been made to the reported data to reflect this effect since the magnitude of the resulting error is well within the assigned uncertainties.

In summary, the primary objective of these measurements has been to obtain data for characterizing the irradiation environment of EBR-II. In August 1971, foil-activation-rate measurements were conducted throughout the core and core-blanket interface region of EBR-II. Comparisons of the mockup data with the EBR-II results will be forthcoming shortly. A more immediate objective of the Assembly 61 experiment was to provide data from which fast-neutron fission yields could be determined. A detailed description of the fission-yield work will be the subject of subsequent reports; however, an overview of this work is presented in Ref. 10. A report on activation-rate measurements in Assemblies 62 and 63 of the EBR-II mockup program conducted in ZPR-3 is now being prepared.

ACKNOWLEDGMENTS

We appreciate the help, discussions, and suggestions of D. Meneghetti, W. Loewenstein, and W. P. Keeney which resulted in the successful completion of this experiment. We specifically acknowledge the encouragement given us by D. Meneghetti and W. Loewenstein to participate in the mockup critical program. R. O. Vosburgh, J. M. Gasidlo, and the operating staff of ZPR-3 were particularly valuable in assisting with loading, irradiating, and removing the samples from the reactor. H. J. Howard and E. D. Duke of SPM provided valuable assistance in handling sample shipments between Chicago and Idaho. We wish also to express our appreciation to several individuals for their effort in various phases of the experiment: J. Williams for her assistance in the preparation, cutting, and mounting of the samples for analysis; R. J. Armani, R. Gold, and J. Roberts for their expertise in the preparation and counting of the mica track recorders and in their use as absolute fission rate monitors; M. T. Laug and G. E. Staahl for their uranium mass-spectrometric isotope-dilution analyses; R. L. Malewicki for assistance in gamma counting; C. L. Blogg for assistance in both track-recorder and gamma counting; and M. S. Foster for support in the area of computer analysis.

REFERENCES

1. N. D. Dudey, R. R. Heinrich, R. J. Popek, R. P. Larsen, and R. D. Oldham. Activation Rate Measurements in the ZPR-3 Mockup Critical Experiments. Part 1. Measurements of Foil-activation Rates and Fission Yields in Assembly 60 of ZPR-3--Mockup of EBR-II with a Uranium Blanket, ANL-7781 (April 1971).

2. W. P. Keeney and R. O. Vosburgh, pp. 31-38 in Reactor Development Progress Report, June 1970, ANL-7705 (July 31, 1970).

3. W. P. Keeney, R. O. Vosburgh, and D. Meneghetti, pp. 32-54 in Reactor Development Program Progress Report, April-May 1970, ANL-7688 (July 14, 1970).

4. W. P. Keeney, R. O. Vosburgh, and D. Meneghetti, pp. 27-34 in Reactor Development Program Progress Report, August 1970, ANL-7737 (Sept. 29, 1970).

5. D. W. Maddison, ibid., pp. 27-34.

6. N. D. Dudey, R. R. Heinrich, R. J. Popek, pp. 92-95 in Reactor Development Program Progress Report, October 1970, ANL-7753 (Nov. 24, 1970).

7. N. D. Dudey, R. R. Heinrich, and R. J. Popek, pp. 53-57 in Reactor Development Program Progress Report, December 1970, ANL-7765 (Jan. 19, 1971).

8. N. D. Dudey, R. J. Popek, and R. R. Heinrich, pp. 1.72-1.76 in Reactor Development Program Progress Report, April-May 1971, ANL-7825 (June 23, 1971).

9. N. D. Dudey, R. J. Popek, and R. R. Heinrich, pp. 1.24-1.27 in Reactor Development Program Progress Report, August 1971, ANL-7854 (Sept. 23, 1971).

10. Chemical Engineering Division Burnup, Cross Sections, and Dosimetry Semiannual Report, July-December 1971, ANL-7899 (in press).

11. M. E. Meek and B. F. Rider, Summary of Fission Product Yields for ^{235}U, ^{238}U, ^{239}Pu, and ^{241}Pu at Thermal, Fission Spectrum, and 14-MeV Neutron Energies, APED-5398 (Mar. 1, 1968).

12. D. Meneghetti, private communication, April 14 and April 21, 1971.

13. George S. Stanford and James H. Sechinger, Thickness Corrections for Neutron-Activated Gold Foils, ANL-7545 (1969).

APPENDIX A

Additions and Improvements to the Reported Assembly 60 Results

Appendix A

Additions and Improvements to the Reported Assembly 60 Results

After the ZPR-3 Assembly 60 results had been published in Ref. 1, several additions and improvements in the reported results were made. One of the major objectives of the Assembly 60 and 61 tests was to measure fast-neutron fission yields by means of the solid-state track-recorder technique. The results from the Assembly 61 experiment enabled us to continue our determinations of fission yields to the point that the values now available are more reliable than those used in the analysis of Assembly 60 data. In addition, a number of absolutely calibrated gamma-ray standards became available which allowed us to calibrate our gamma-ray detectors more accurately. With both of these improvements now being available, it is possible to correct the reported Assembly 60 results.

Table A-I summarizes the corrected absolute fission and reaction rates measured in the dosimetry foils in the Assembly 60 irradiation. Table A-II lists the corrected absolute fission rates measured in the fission-yield samples. Table A-III summarizes the drawer-averaged fission and reaction rates for the dosimetry (D), fission-yield (Y), and Applied Physics Group foil sets[5] corrected to reflect both the fission-yield and detector efficiency changes.

At the time the report on the Assembly 60 experiment (Ref. 1) was prepared, analysis of the solid-state track recorders had not been completed. The track recorders have now been counted and the number of atoms of fissile material exposed to each track recorder has been determined. The results for the number of fissions per nanogram of fissile material and the deduced fission rates for ^{235}U, ^{238}U, and ^{239}Pu are tabulated in Table A-IV. Also given in this table are the mica track-recorder numbers. (The sample weights, irradiation position, and other details are given in Ref. 1.) The massive samples adjacent to each track recorder during the irradiation are also identified in Table A-IV.

TABLE A-I. Corrected Assembly 60 Absolute Fission and Reaction Rates From Dosimetry Packets

	Sample	Rate $[10^{-16}$ atoms/(atom)(sec)]				
		$^{235}U(n,f)$	$^{238}U(n,f)$	$^{238}U(n,\gamma)$	$^{197}Au(n,\gamma)$	$^{58}Ni(n,p)$
Blanket	1	127	2.15	17.0	36.4	0.505
	2	157	2.61	19.8	40.0	0.603
	3	162	3.22	22.9	42.8	0.720
	4	184	3.87	22.4	44.7	0.933
Interface	1	279	13.9	30.9	61.1	3.68
	2	287	14.3	29.9	57.2	3.87
	3	300	17.4	32.2	57.3	4.35
	4	307	18.0	34.4	60.0	4.59
	5	310	20.5	35.4	61.0	5.17
	6	314	21.5	35.1	60.7	5.72
	7	340	21.7	34.2	61.4	5.97
	8	343	21.8	37.9	62.4	5.57
Core	1	478	33.2	45.1	84.2	8.93
	2	487	33.3	44.9	85.9	9.03
	3	500	35.1	46.4	82.7	9.40
	4	483	33.1	48.7	84.9	9.12
	5	490	32.4	43.7	85.2	9.38
	6	502	34.8	46.5	84.2	9.78
	7	509	37.2	45.3	83.8	9.97
	8	516	35.3	44.8	85.1	9.25
	11	502	33.6	45.9	82.7	9.11
	12	483	32.4	44.3	85.1	9.25
	13	502	37.2	47.7	85.7	9.64
	14	483	35.1	46.5	86.0	9.41
	15	497	35.3	46.8	86.3	9.59
	16	506	35.7	48.2	85.5	10.09
	17	509	38.1	47.7	86.7	10.26
	18	506	35.7	48.4	86.4	9.47
	21	502	33.9	45.8	81.6	9.22
	22	497	33.9	46.5	85.4	9.27
	23	500	36.0	46.4	83.3	9.64
	24	487	33.9	45.3	87.1	9.31
	25	490	34.5	48.8	87.3	9.59
	26	516	36.0	46.1	84.2	10.07
	27	512	37.7	47.9	88.3	10.24
	28	512	35.3	48.4	88.0	9.51

TABLE A-II. Corrected Assembly 60 Absolute Fission Rates of ^{235}U, ^{238}U, and ^{239}Pu Determined From Fission-yield Packets

Sample		Fission Rate [10^{-16} fissions/(atom)(sec)]		
		$^{235}U(n,f)$	$^{238}U(n,f)$	$^{239}Pu(n,f)$
Core	1	475	31.0	572
	2	459	31.8	560
	3	459	30.2	554
	4	453	30.4	560
	5	452	30.5	562
	6	454	31.2	563
	7	-	-	572
Interface	1	321	18.3	
	2	303	17.9	
	3	300	16.5	
	4	294	15.9	
	5	289	15.2	
	6	282	15.1	
Blanket	1	178		199
	2	173		187
	3	167		179
	4	159		169
	5	157		163
	6	150		157
	7	-		153

TABLE A-III. Corrected Assembly 60 Drawer-averaged Fission and Reaction Rates Determined at the Core, Interface, and Blanket Locations for the D, Y, and A Packets

	Reactor Position	Foil Packet	Reaction Rate [10^{-16} atoms/(atom)(sec)]					
			$^{235}U(n,f)$	$^{238}U(n,f)$	$^{239}Pu(n,f)$	$^{238}U(n,\gamma)$	$^{197}Au(n,\gamma)$	$^{58}Ni(n,p)$
Core	0-15	D	497	34.8	-	44.6	85.5	9.48
	0-17	Y	459	30.9	563	46.7	-	-
	Q-15	A[a]	522	36.4	-	47.9	73.7	9.59
Interface	0-11	D	312	19.0	-	34.4	60.2	4.89
	0-21	Y	298	16.5	-	32.4	-	-
	Q-11	A[a]	332	19.4	-	30.8	50.8	5.17
Blanket	0-9	D	160	3.07	-	21.1	41.6	0.71
	0-23	Y	164	-	172	-	-	-
	Q-9	A[a]	173	2.63	-	19.6	36.9	0.68

[a]Data taken from Ref. 5 and converted to above units.

TABLE A-IV. Assembly 60 Absolute Fission Rates of ^{235}U, ^{238}U, and ^{239}Pu Measured by the Solid-state Track Recorders

Sample Location[a]		$^{235}U(n,f)$			$^{238}U(n,f)$			$^{239}Pu(n,f)$		
		Sample Number	Fiss/ng	Rate x10^{16}	Sample Number	Fiss/ng	Rate x10^{16}	Sample Number	Fiss/ng	Rate x10^{16}
Core	1	-						1-4	440	477
	2	14-1	395	421	-			4-1	459	498
	3	13-3	407	434	8-3	26.8	28.9	1-3	518	562
	4	14-2	430	458	7-2	27.1	29.3	4-2	516	559
	5	13-2	427	455	8-2	27.2	29.4	1-2	511	554
	6	14-3	408	435	7-3	27.5	29.7	4-3	472	512
	7	13-1	387	413	8-1	27.3	29.5	1-1	481	521
	7				7-4	26.5	28.6			
Interface	1	15-4	282	301	10-4	11.4	12.3	-		
	2	-			9-1	12.1	13.1	6-1	318	345
	3	15-3	271	289	10-3	13.3	14.4	-		
	4	-			9-2	14.0	15.1	6-2	299	324
	5	15-2	244	260	10-2	15.2	16.4	-		
	6	16-3	243	250	9-3	16.2	17.5	6-3	293	318
	7	15-1	242	258	10-1	16.2	17.5	6-4	276	299
	7				9-4	16.2	17.5			
Blanket	1	17-4	153	163				2-4	144	156
	2	18-1	150	160				3-1	156	169
	3	-						2-3	148	160
	4	18-2	138	147				3-2	145	157
	5	-						2-2	139	151
	6	-						3-3	137	149
	7	17-1	121	129				2-1	131	142
	7							3-4	126	137

[a]Number of massive sample associated with given track recorder.